# Highly Efficient, Iodine-Free Dye-Sensitized Solar Cells with Solid-State Synthesis of Conducting Polymers

**ARTICLE** *in* ADVANCED MATERIALS · APRIL 2011

Impact Factor: 17.49 · DOI: 10.1002/adma.201004715 · Source: PubMed



**5 AUTHORS**, INCLUDING:

Jeonghun Kim
University of Wollongong
**44** PUBLICATIONS **566** CITATIONS
SEE PROFILE

Byeonggwan Kim
Yonsei University
**37** PUBLICATIONS **490** CITATIONS
SEE PROFILE

Jong Hak Kim
Yonsei University
**284** PUBLICATIONS **4,101** CITATIONS
SEE PROFILE

Eunkyoung Kim
Yonsei University
**210** PUBLICATIONS **2,948** CITATIONS
SEE PROFILE

# Highly Efficient, Iodine-Free Dye-Sensitized Solar Cells with Solid-State Synthesis of Conducting Polymers

*Jong Kwan Koh, Jeonghun Kim, Byeonggwan Kim, Jong Hak Kim,* and Eunkyoung Kim**

Dye-sensitized solar cells (DSSCs) are low-cost photovoltaic devices that provide a high energy conversion efficiency of 11%.[1] High conversion efficiency, good stability, and easy fabrication are essential for commercialization of DSSCs.[2] Although DSSCs with liquid electrolytes have been reported to exhibit high efficiency, there has been interest in developing a solid-state DSSC (ssDSSC) due to its potential to decrease the overall weight of the cells and to provide long-term durability and flexibility. Several methods have been developed to fabricate ssDSSCs employing quasi-solid or solid polymer electrolytes.[3–11]

In ssDSSCs, hole transporting materials (HTMs) and the control of interfacial properties between the nanoporous $TiO_2$ layer and the HTM are critical to the photoconversion efficiency of the cells. Recently, HTMs have been extensively investigated as potential replacements for conventional $I_3^-/I^-$ redox electrolyte systems using iodine ($I_2$) in DSSCs.[12–18] As an organic HTM, spiro-OMeTAD was used for an iodine free ssDSSC and showed higher efficiency of 5.1%.[17,18] Inorganic HTMs such as CuI showed a good efficiency of 4.7%,[12] but the crystal formation of metal oxide gradually reduced cell performance.[19] Another possibility is the utilization of p-type conducting polymers, e.g., polypyrrole, polyaniline, polydiacetylene, poly (3-octylthiopehene), and poly(3,4-ethylenedioxythiophene) (PEDOT).[20–26] These polymers are advantageous over other small molecules due to their low cost, good stability, simple fabrication using spin-coating, and easy preparation of designable structures. Recently, Ho et al. reported an iodine ($I_2$)-free ssDSSC using polyaniline/carbon black composite with imidazolium iodide derivatives, which effectively generates $I^-/I_3^-$ redox couples without addition of iodine ($I_2$).[27] However, while conductive polymers offer many advantages, they show low energy conversion efficiencies due to poor penetration into the nanopores of $TiO_2$ photoelectrodes that arises from mismatches between the molecular sizes of the polymers and the pore sizes of the $TiO_2$ layer.

Recently, Yanagida et al. were successful at improving the power conversion efficiency significantly up to 2.85%, which was the highest efficiency for an iodine-free ssDSSC using a conductive polymer as HTM.[28–30] The penetration of a conductive polymer into $TiO_2$ porous layers was successfully improved via the in situ photoelectrochemical polymerization of a heterocyclic monomer, e.g., 2,2'-bis(3,4-ethylenedioxythiophene) (bis-EDOT).[29] However, the maximum penetration depth of the conductive polymer into the $TiO_2$ layer was 4–5 μm, above which cell efficiency was decreased, resulting from insufficient interfacial properties of electrode/HTM despite increased dye adsorption. More recently, Liu et al. further improved cell efficiency up to 6.1% using indoline D149 dye as a sensitizer,[31] where in situ photoelectropolymerization of bis-EDOT was also utilized. However, the maximum efficiency of Z907-sensitized devices was 1.7% at 4.2 μm, above which the cell efficiency sharply decreased, e.g., 0.3% at 9.4 μm.

In addition to the constraint of the penetration depth, the photoelectrochemical polymerization method has another limitation, i.e., the selection of the dye and monomer, wherein the oxidation potential for the polymerization reaction should be matched. Furthermore, the photoelectrochemical polymerization process is complex and therefore undesirable for large-scale commercialization. In this work, we report an advantageous preparation method for ssDSSCs with higher efficiency and improved interfacial properties using in situ solid state polymerization (SSP) of a conducting polymer.

SSP, which yields highly conductive polymers, has been reported using halogenated crystalline heterocyclic monomers.[32] This method provides a facile polymerization reaction initiated by heating and results in a highly ordered crystalline polymer. In this work, a brominated 3,4-ethylenedioxythiophene was selected as a solid-state polymerizable monomer for synthesis of the conductive polymer due to its low cost of preparation, ease of synthesis, effective polymerization, and the commercial availability of 3,4-ethylenedioxythiophene (EDOT). Thus a dibromo-EDOT (DBEDOT) was synthesized with a high yield (≈76%) via the common bromination method, as confirmed by $^1$H NMR spectroscopy (**Figure 1**a). The synthesized crystalline monomer (DBEDOT) showed good solubility in many common solvents and was polymerizable in the solid state upon heating. The SSP of DBEDOT occurs only in the crystal state due to the short Br···Br distance between monomers.[32] The specific stacking structure of DBEDOT crystals allows the monomer to undergo a coupling self-reaction, leading to the formation of highly conductive PEDOT. The crystal DBEDOT is small enough to penetrate into the nanopores of nanocrystalline $TiO_2$ layers where SSP occurs upon heating without additives. Solid-state polymerized PEDOT (ssPEDOT) showed a crystal form with the original dark color of PEDOT (Figure 1a). The conductivity of the ssPEDOT without any additives reached high conductivity of 9.3 S cm$^{-1}$ at room temperature, which is about 5300 times higher than the value for PEDOT that was chemically polymerized with $FeCl_3$ ($1.7 \times 10^{-3}$ S cm$^{-1}$). Such a high conductivity of ssPEDOT could be contributed to the doping with $Br_3^-$ during polymerization,[32]

J. K. Koh, J. Kim, B. Kim, Prof. J. H. Kim, Prof. E. Kim
Department of Chemical and Biomolecular Engineering
Yonsei University
262 Seongsanno, Seodaemun-gu, Seoul 120–749, South Korea
E-mail: jonghak@yonsei.ac.kr; eunkim@yonsei.kr

**DOI: 10.1002/adma.201004715**

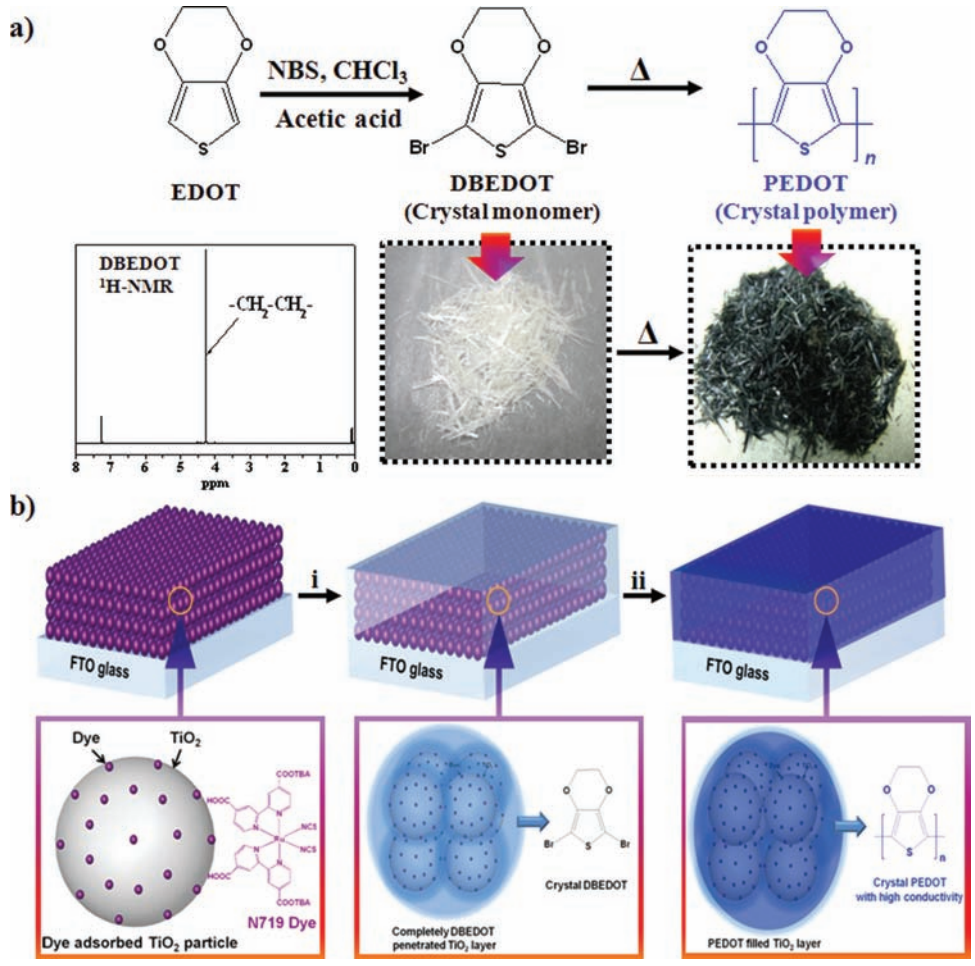


**Figure 1.** Schematic representation for a) the synthesis of solid-state polymerizable 2,5-dibromo-EDOT (DBEDOT) and b) the facile fabrication process for highly efficient iodine-free ssDSSC using N719 dye and conductive polymer as HTM. i) Complete penetration of solid polymerizable monomer through the dropping and drying of the DBEDOT solution. ii) SSP process for the preparation of highly conductive polymer at a proper temperature and time (see Experimental Section for details).

therefore, ssPEDOT with high conductivity can be a good candidate as a HTM.

The in situ SSP method was applied to the preparation of iodine-free ssDSSCs (Figure 1b). In particular, a two-step casting method was carried out to maximize the interfacial properties between the electrode and HTM. First, a dilute solution of DBEDOT (1 wt% in ethanol) was cast onto a N719 dye-adsorbed $TiO_2$ electrode and then, successively, a more concentrated solution (3 wt%) of DBEDOT was casted. After controlled evaporation of the solvent, the $TiO_2$ photoelectrode was placed in an oven at 60 °C, by which the SSP of DBEDOT occurs under atmosphere. ssPEDOT was synthesized at 60 °C, because the conductivity of PEDOT tends to be high when polymerized at lower temperature.[32]

The effect of temperature on the SSP rate was examined over a wide range of temperatures. DSC studies for DBEDOT powder (DBEDOT-pw) and DBEDOT penetrated $TiO_2$ (DBEDOT-$TiO_2$) films revealed that reactions carried out at higher temperatures induced higher polymerization rates in both samples in isothermal DSC measurements (Figure S3a,b, Supporting Information). The DBEDOT-pw samples showed slightly faster polymerization rate than the DBEDOT-$TiO_2$ film, possibly due to delayed kinetics in the latter. However, the activation energy for DBEDOT-pw (24.4 ± 0.8 kcal mol$^{-1}$, $R^2$ = 0.997, where $R^2$ is the accuracy of fitting) was not significantly different from that for DBEDOT penetrated $TiO_2$ film (26.0 ± 2.3 kcal mol$^{-1}$, $R^2$ = 0.977), as determined from the slopes in Figure S3c (Supporting Information) using the Arrhenius equation shown in Equation (1):

$$\ln k = \ln(1/t_{1/2}) = \ln A - (E_a/RT) \quad (1)$$

where the half-time for full conversion ($t_{1/2}$) was taken as a point of 50% release of the heat, in which the position of the exothermic peaks depends on the reaction temperature. The similarities of these activation energies show that the SSP of DBEDOT is not greatly affected by the presence of nanoporous $TiO_2$ films.

Successful penetration of DBEDOT and SSP was also confirmed using Fourier transform infrared (FTIR) spectroscopy (Figure S1 and Table S1, Supporting Information) and X-ray diffraction (XRD) measurements (Figure S3d, Supporting

Information). The peaks of pristine $TiO_2$, DBEDOT, and ssPEDOT exhibited good agreement with previous reports.[33] After SSP of DBEDOT, the ssPEDOT spectrum showed vibrational peaks in the range of 1540 and 1485 $cm^{-1}$ originating from the conjugated C=C asymmetric and symmetric stretching vibration in the thiophene ring, respectively.[33] The IR absorption peaks of the PEDOT-penetrated $TiO_2$ film mirrored those of pristine PEDOT and $TiO_2$, indicating that DBEDOT was successfully penetrated and polymerized in the $TiO_2$ layer. The peaks of crystalline DBEDOT, crystalline ssPEDOT, and anatase $TiO_2$ film were confirmed by XRD with good agreement with previous reports.[32,34–36] The XRD patterns of PEDOT-penetrated $TiO_2$ were not significantly different from those of pristine $TiO_2$ and crystalline ssPEDOT.

In ssDSSCs, a high level of interfacial contact between the dye-adsorbed $TiO_2$ layer and HTM is of pivotal importance in enhancing the energy conversion efficiency. The surface and cross-sectional scanning electron microscopy (SEM) images of nanoporous $TiO_2$ films before and after the penetration of the monomer and SSP are shown in **Figure 2** and Figure S2 (Supporting Information). $TiO_2$ nanoparticles were distinguishable with a size of 30–40 nm in the pristine nanoporous $TiO_2$ layer (Figure 2a) and $TiO_2$ layer had about 17-nm pore size, which was determined using the Brunauer–Emmett–Teller (BET) measurement.[37] The pore size was large enough that the dilute DBEDOT solution could effectively penetrate to the $TiO_2$ layer pores. When DBEDOT was penetrated and polymerized at 60 °C in the solid-state, the $TiO_2$ particle size apparently increased, and the images of the nanoparticles became indistinct (Figure 2b). This occurred because $TiO_2$ nanoparticles are covered by ssPEDOT, indicating excellent contact between the dye-adsorbed $TiO_2$ particles and ssPEDOT. Good penetration of DBEDOT into the nanopores of $TiO_2$ and SSP, and thus better interfacial contact, are possible because DBEDOT has a smaller molecular size than the pores of the $TiO_2$ layer. This approach provides a simple but effective method for filling a large molecular weight conductive polymer into the nanopores of a $TiO_2$ film as the HTM. The pores of the $TiO_2$ film were additionally filled with lithium bistrifluoromethanesulfonimide (LiTFSI) and 1-methyl-3-propyl-imidazolium iodide (MPII), indicating further improvement of interfacial contact between the photoelectrode and the HTM (Figure 2c). The improved interfacial properties between the nanoporous $TiO_2$ film and the ssPEDOT were also supported by transmission electron microscopy (TEM) images. As shown in Figure 2d,e, the porous $TiO_2$ film became completely packed with ssPEDOT (black brush). The pores as well as inside $TiO_2$ nanoparticles were interweaved by the ssPEDOT to result in borderless morphology. Importantly, this method allows the conducting polymer PEDOT to deeply penetrate into the nanopores of a 11-μm-thick $TiO_2$ film to the bottom as shown in Figure 2f. This effective penetration of HTM to the bottom of the $TiO_2$ film should be very encouraging as it gives the higher performance of the ssDSSC, as described below. Furthermore this explains why this method has athe

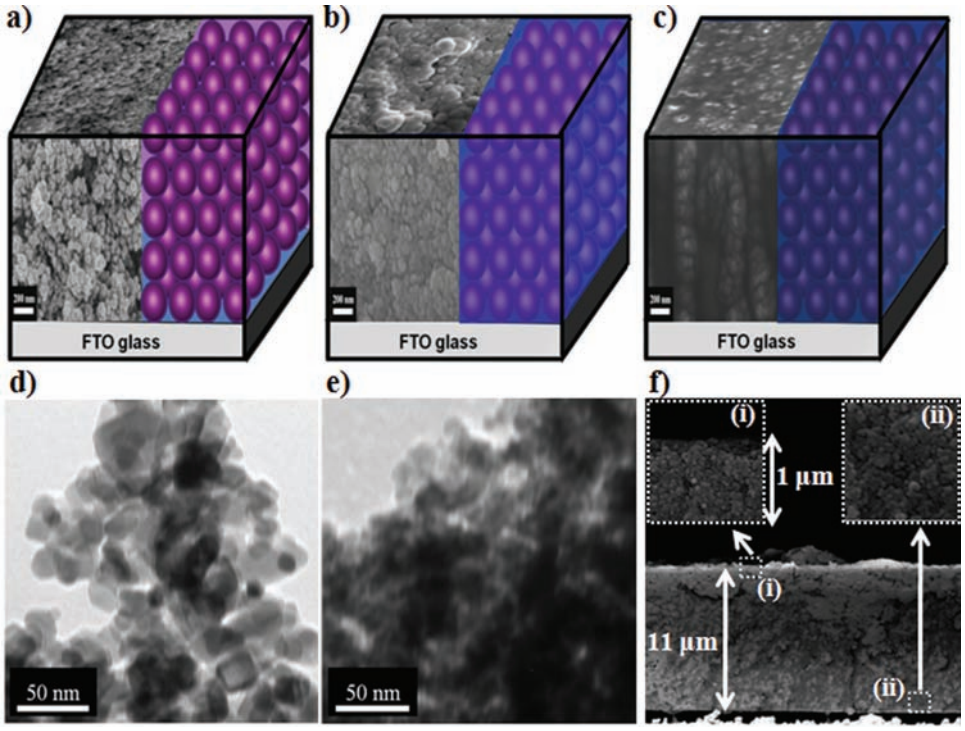


**Figure 2.** Electron microscopy images of dye-sensitized $TiO_2$ photoelectrodes. In the three SEM images (a–c), left parts are high-resolution (HR)-SEM images of the cross-section and surface of photoelectrode and the right parts are the representative schemes of photoelectrode according to fabrication steps. a) After N719 dye adsorption, b) after dropping and penetration of DBEDOT onto (a) and SSP at 60°C, and c) after addition of additives. d,e) TEM images of pristine $TiO_2$ and PEDOT-penetrated $TiO_2$ after SSP, respectively. f) HR-SEM images of cross-section of (b) in full-film-thickness scale and the magnified images of i) the surface and ii) the bottom layer are shown as insets (dotted box).

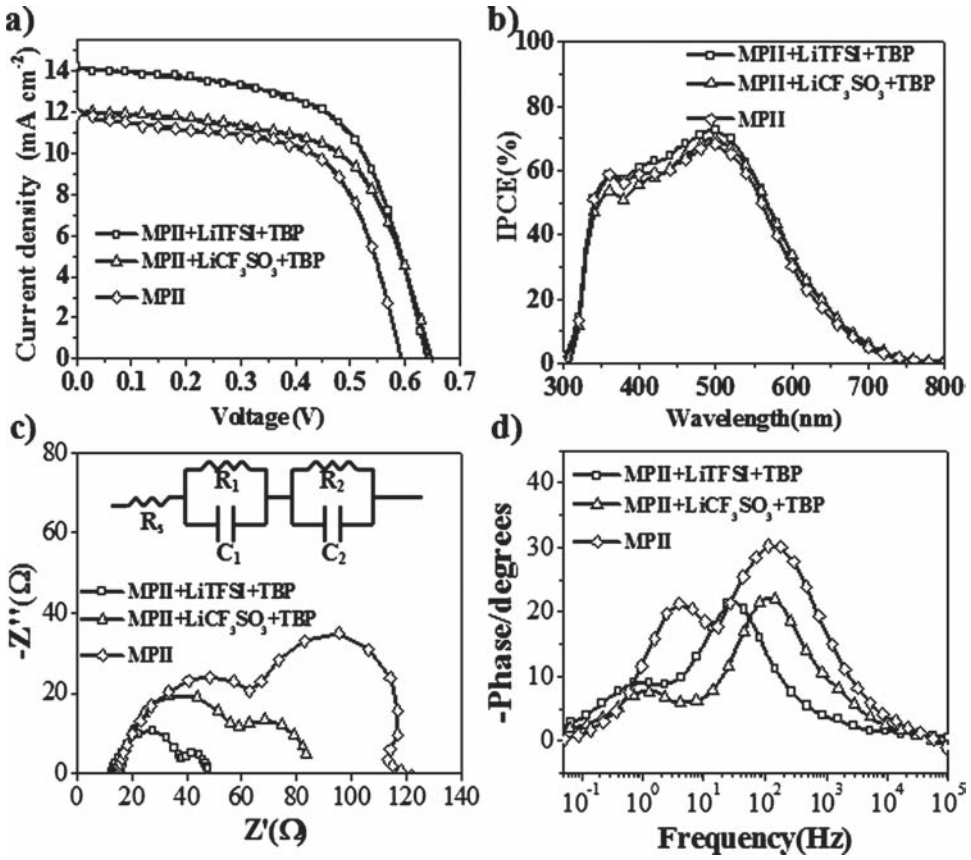


**Figure 3.** Cell performances of iodine-free ssDSSC and electrical impedance spectroscopy (EIS) analysis. a) Current–voltage (*J–V*) curves of iodine-free ssDSSCs with various additives at 100 mW cm$^{-2}$. b) IPCE of each device. c) Nyquist plots of the iodine-free ssDSSC and d) Bode phase plots of each device.

dvantages of deep penetration and high performance compared with the photoelectrochemical polymerization method, which has been limited to achieve good pore filling due to solution-state polymerization.[28–30]

As shown in **Figure 3**a,b, the photovoltaic performance and the corresponding incident photon-to-current efficiency (IPCE) spectra for devices were largely dependent on the doping anion, resulting from differences in the charge transfer rate, mobility, and charge delocalization of ions:[20,29] MPII/LiTFSI/TBP > MPII/$LiCF_3SO_3$/TBP > MPII. 4-*tert*-butylpyridine (TBP) was additionally introduced because it can prevent the dark current and shift the conduction band edge level of $TiO_2$ to negative due to its basicity, leading to an improvement in the open circuit voltage ($V_{oc}$).[38,39] The best performance (i.e., 5.4%) was obtained for the DSSC fabricated using PEDOT doped with LiTFSI/TBP, which is, to the best of our knowledge, the highest efficiency for a N719 dye based $I_2$-free ssDSSC. Similarly, the cell using LiI showed good performance as shown in the MPII system (Figure S4 and Table S2, Supporting Information). Upon using other ionic liquids, such as 1-ethyl-3-methylimidazolium chloride, 1-ethyl-3-methylimidazolium bromide, and 1-ethyl-3-methylimidazolium bis (trifluoromethyl sulfonyl) imide, however, the DSSCs showed poor performances. It indicates that the $Br_3^-$ anion doped on ssPEDOT did not react with $Br^-$, $Cl^-$, or $CF_3SO_3^-$ for a redox couple but played a role as a dopant of ssPEDOT. According to a recent report,[27] a conducting polymer or carbon material can function as a charge transfer mediator when using ionic liquids containing iodide anion. It suggests that the iodide anion ($I^-$) of MPII functions as an electron transfer whereas ssPEDOT works as a charge transfer media.

An IPCE value as high as 72.6% at 500 nm was obtained for the MPII/LiTFSI/TBP system, which is 10% higher than that obtained with photoelectrochemically polymerized PEDOT.[29] The remarkably improved efficiency observed in the present study results from the utilization of in situ SSP of highly conductive PEDOT, by which the small DBEDOT monomers can deeply penetrate into the nanopores of a thick nanocrystalline $TiO_2$ layer. It should be noted that the maximum penetration depth of a conductive polymer is about 4–5 μm when using photoelectrochemical polymerization, leading to lower dye adsorption and cell efficiency.[29,31]

Electrochemical impedance spectroscopy (EIS) was used to characterize the internal resistance and charge-transfer kinetics of nanocrystalline $TiO_2$ layers, as shown in Figure 3c,d. An applied bias of $V_{oc}$ at a frequency range from 0.05 Hz to 0.1 MHz was used, with an AC amplitude of 0.02 V and a light intensity of 100 mW cm$^{-2}$. Electrochemical para-meters determined from EIS analysis, resistance values, minimum angular frequency ($\omega_{min}$), and lifetime of electrons for

**Table 1.** Performances and EIS results of iodine-free ssDSSCs fabricated with ssPEDOT at 100 mW cm$^{-2}$. $J_{sc}$ = current density; FF= fill factor.

| Additives | $V_{oc}$ (V) | $J_{sc}$ (mA cm$^{-2}$) | FF | Efficiency (%) | $R_s$ | $R_1$ | $R_2$ | $\omega_{min}$ (Hz) | $\tau_r$ (ms) |
|---|---|---|---|---|---|---|---|---|---|
| MPII | 0.60 | 11.9 | 0.61 | 4.3 | 14.3 | 62.8 | 118.8 | 122.5 | 8.1 |
| MPII+$LiCF_3SO_3$+TBP | 0.65 | 12 | 0.61 | 4.7 | 14.3 | 60.4 | 84.2 | 118.3 | 8.5 |
| MPII+LiTFSI+TBP | 0.64 | 14.2 | 0.60 | 5.4 | 12.7 | 37.9 | 48.1 | 33.1 | 30.2 |

recombination ($\tau_r$) are summarized in **Table 1**. Each equivalent circuit consisted of three components: ohmic resistance ($R_s$), charge transfer resistance at counter electrode/HTM ($R_1$), and charge transfer resistance at the photoelectrode/HTM ($R_2$) interface. The results show that the DSSC fabricated using MPII/LiTFSI/TBP exhibited the smallest $R_1$, indicating faster charge transport at the interface of Pt/ssPEDOT. In addition, the $R_2$ value of the MPII/LiTFSI/TBP system was the lowest, representing low resistance to charge transfer between PEDOT/$TFSI^-$ and the $TiO_2$/dye. According to the EIS model, the effective electron lifetime before recombination ($\tau_r$) in the $TiO_2$ photoelectrode can be estimated from the minimum angular frequency ($\omega_{min}$) value of the impedance semicircle at middle frequencies in the Bode spectrum: $\tau_r = 1/\omega_{min}$. The electrons lifetime for recombination ($\tau_r$) for the MPII/LiTFSI/TBP system was the highest value, 30.2 ms. This could effectively decrease electron recombination, leading to significantly enhanced electron transfer and further improved cell performance. Based on this result, the DSSC fabricated using ssPEDOT with MPII/LiTFSI/TBP is suitable for iodine-free ssDSSC applications. In the measurement of chemical capacitance ($C_\mu$) as a function of bias voltage, the $C_\mu$ values of N719-sensitized DSSCs employing LiTFSI and $LiCF_3SO_3$ were lower than those of DSSC employing MPII. This indicates that the energy gap between the $TiO_2$ conduction-band edge and the PEDOT Fermi level is larger for N719-sensitized DSSCs employing LiTFSI and $LiCF_3SO_3$ than that for DSSC employing MPII (Figure S5, Supporting Information).[31] In general, TBP adsorption onto the $TiO_2$ surface shifts the conduction band edge level of $TiO_2$ negatively due to the basicity of TBP, which results in improved $V_{oc}$.[40]

In summary, a facile method for the preparation of iodine-free ssDSSC with excellent performance and improved electrode/HTM interfacial properties based on the SSP of a conductive polymer was developed. The solid-state polymerizable monomer was small enough to effectively penetrate into the nanopores of $TiO_2$ film, improving interfacial contact between the electrode and HTM. Importantly, this approach allowed deep penetration of HTM into an 11-μm-thick $TiO_2$ film, allowing for enhanced dye adsorption and resulting in high performance. The cell fabricated using the PEDOT/MPII/LiTFSI/TBP system exhibited an effective electron lifetime of 30.2 ms and an excellent energy conversion efficiency of 5.4%, which is the highest value in iodine-free ssDSSCs with N719 dye. We believe that this SSP approach introduces a new and simple route toward the synthesis of conducting polymer as the HTM in iodine-free ssDSSCs serves as an alternative to the conventional photoelectrochemical polymerization method.

## Experimental Section

The ssDSSCs were constructed by drop-casting electrolyte solution onto the photoelectrode and covering with a Pt-coated counter electrode, using the previously reported procedure.[34–37] Transparent $SnO_2$/F-layered conductive glass (FTO, Pilkington. Co. Ltd., 8 Ω □$^{-1}$) was used to prepare the photoelectrode. The photoelectrode was fabricated by spin coating (at 2000 rpm) a solution of titanium bis(ethyl acetoacetate) diisopropoxide (0.15 M) in butanol onto the FTO (fluorine-doped tin oxide) glass followed by heating at 450 °C for 30 min. The commercial $TiO_2$ paste (solaronix D20) was casted onto the glass using a doctor-blade technique, followed by successive sintering at 450 °C for 30 min. Nanocrystalline $TiO_2$ films were immersed into N719 solution (0.5 mM in ethanol) for 24 h at room temperature. The DBEDOT was dissolved in anhydrous ethanol (1 wt% and 3 wt%) and a few drops of the solution were directly casted onto the $TiO_2$ photoelectrode and counter electrode. After drying the solvent, the DBEDOT onto the photoelectrode was thermally polymerized at 60 °C for 24 h in an oven. Then, a drop of the acetonitrile solution consisting of MPII (1.0 M), TBP (0.2 M), and Li salt (0.2 M) was casted onto the photoelectrode. After evaporation of the solvent in a vacuum oven, sandwich-type DSSCs were fabricated by clipping two electrodes. The active area was 0.16 cm$^2$. Photoelectrochemical performance characteristics were measured using a electrochemical workstation (Keithley Model 2400) and asolar simulator (1000 W xenon lamp, Oriel, 91193). The light was homogeneous over an 8 in. × 8 in. area and was calibrated with a Si solar cell (Fraunhofer Institute for Solar Energy System, Mono-Si+KG filter, Certificate No. C-ISE269) to a sun light intensity of 1 (100 mW cm$^{-2}$). This calibration was double-checked with a NREL-calibrated Si solar cell (PV Measurements Inc.). Incident photon-to-current efficiency (IPCE) measurement was carried out using a 300 W Xe light source and a monochromator (Polaronix K3100 IPCE Measurement System, McScience).

## Supporting Information

Supporting Information is available from the Wiley Online Library or from the author.

## Acknowledgements

J.K.K. and J.K. contributed equally to this work. The authors acknowledge the financial support of a Ministry of Knowledge Economy (MKE), National Research Foundation (NRF) grant funded by the Korean government (MEST) through the Active Polymer Center for Pattern Integration (R11–2007-050–00000-0) and the Korea Center for Artificial Photosynthesis (KCAP) (NRF-2009-C1AAA001–2009-0093879).

Received: December 24, 2010
Published online: February 18, 2011

[1] B. O'Regan, M. Grätzel, *Nature* **1991**, *353*, 737.
[2] F. Sauvage, D. H. Chen, P. Comte, F. Z. Huang, L. P. Heiniger, Y. B. Cheng, R. A. Caruso, M. Grätzel, *ACS Nano* **2010**, *4*, 4420.

[3] T. C. Li, M. S. Goes, F. Fabregat-Santiago, J. Bisquert, P. R. Bueno, C. Prasittichai, J. T. Hupp, T. J. Marks, *J. Phys. Chem. C* **2009**, *113*, 18385.
[4] S. Yanagida, Y. H. Yu, K. Manseki, *Acc. Chem. Res.* **2009**, *42*, 1827.
[5] J. B. Xia, N. Masaki, M. Lira-Cantu, Y. Y. Kim, K. J. Jiang, S. Yanagida, *J. Phys. Chem. C* **2008**, *112*, 11569.
[6] J. G. Chen, C. Y. Chen, C. G. Wu, K. C. Ho, *J. Phys. Chem. C* **2010**, *114*, 13832.
[7] K. C. Huang, Y. C. Wang, R. X. Dong, W. C. Tsai, K. W. Tsai, C. C. Wang, Y. H. Chen, R. Vittal, J. J. Lin, K. C. Ho, *J. Mater. Chem.* **2010**, *20*, 4067.
[8] J. N. Freitas, A. S. Gonçalves, M. A. Paoli, J. R. Durrant, A. F. Nogueira, *Electrochim. Acta* **2008**, *53*, 7166.
[9] J. E. Benedetti, M. A. Paoli, A. F. Nogueira, *Chem. Commun.* **2008**, *9*, 1121.
[10] H. Han, W. Liu, J. Zhang, X. Z. Zhao, *Adv. Funct. Mater.* **2005**, *15*, 1940.
[11] N. Fukuri, N. Masaki, T. Kitamura, Y. Wada, S. Yanagida, *J. Phys. Chem. B* **2006**, *110*, 25251.
[12] G. Kumara, M. Okuya, K. Murakami, S. Kaneko, V. Jayaweera, K. Tennakone, *J. Photochem. Photobiol. A* **2004**, *164*, 183.
[13] B. O'Regan, D. T. Schwartz, S. M. Zakeeruddin, M. Grätzel, *Adv. Mater.* **2000**, *12*, 1263.
[14] H. J. Snaith, M. Grätzel, *Appl. Phys. Lett.* **2006**, *89*, 262114.
[15] M. Nedelcu, J. W. Lee, E. J. W. Crossland, S. C. Warren, M. C. Orilall, S. Guldin, S. Hüttner, C. Ducati, D. Eder, U. Wiesner, U. Steiner, H. J. Snaith, *Soft Matter* **2009**, *5*, 134.
[16] P. Chen, J. Yum, F. Angelis, E. Mosconi, S. Fantacci, S. Moon, R. Baker, J. Ko, M. Nazeeruddin, M. Grätzel, *Nano Lett.* **2009**, *9*, 2487.
[17] H. Snaith, A. Moule, C. Klein, K. Meerholz, R. Friend, M. Grätzel, *Nano Lett.* **2007**, *7*, 3372.
[18] J.-H. Yum, P. Chen, M. Grätzel, M. K. Nazeeruddin, *ChemSusChem* **2008**, *1*, 699.
[19] P. M. Sirimanne, T. Jeranko, P. Bogdanoff, S. Fiechter, H. Tributsch, *Semicond. Sci. Technol.* **2003**, *18*, 708.
[20] J. Wu, S. Hao, Z. Lan, J. Lin, M. Huang, Y. Huang, P. Li, S. Yin, T. Sato, *J. Am. Chem. Soc.* **2008**, *130*, 11568.
[21] D. Gebeyehu, J. B. Crabec, N. S. Sariciftci, D. Vangeneugden, R. Kiebooms, D. Vanderzande, F. Kienberger, H. Schindler, *Synth. Met.* **2002**, *125*, 279.
[22] S. A. Haque, T. Park, C. Xu, S. Koops, N. Schulte, R. J. Potter, A. B. Holmes, J. R. Durrant, *Adv. Funct. Mater.* **2004**, *14*, 435.
[23] C. D. Grant, A. M. Schwartzberg, G. P. Smestad, J. Kowalik, L. M. Tolbert, J. Z. Zhang, *J. Electroanal. Chem.* **2002**, *522*, 40.
[24] K. J. Jiang, K. Manseki, Y. H. Yu, N. Masaki, J. B. Xia, L. M. Yang, Y. L. Song, S. Yanagida, *Adv. Funct. Mater.* **2009**, *19*, 2481.
[25] R. Zhu, C. Y. Jiang, B. Liu, S. Ramakrishna, *Adv. Mater.* **2009**, *9*, 994.
[26] S. Tan, J. Zhai, B. Xue, M. Wan, Q. Meng, Y. Li, L. Jiang, D. Zhu, *Langmuir* **2004**, *20*, 2934.
[27] C.-P. Lee, P.-Y. Chen, R. Vittala, K.-C. Ho, *J. Mater. Chem.* **2010**, *20*, 2356.
[28] R. Senadeera, F. Norihiro, Y Saito, T. Kitamura, Y. Wada, S. Yanagida, *Chem. Commun.* **2005**, *17*, 2259.
[29] J. B. Xia, N. Masaki, N. Lira-Cantu, Y. Kim, K. J. Jiang, S. Yanagida, *J. Am. Chem. Soc.* **2008**, *130*, 1258.
[30] K. J. Jiang, K. Manseki, Y. H. Yu, N. Masaki, K. Suzuki, Y. L. Song, S. Yanagida, *Adv. Funct. Mater.* **2009**, *19*, 2481.
[31] X. Liu, W. Zhang, S. Uchida, L. Cai, B. Liu, S. Ramakrishna, *Adv. Mater.* **2010**, *22*, E150.
[32] H. Meng, D. F. Perepichka, M. Bendikov, F. Wudl, G. Z. Pan, W. Yu, A, S. Brown, *J. Am. Chem. Soc.* **2003**, *125*, 15151.
[33] J. Kim, J. You, E. Kim, *Macromolecules* **2010**, *43*, 2322.
[34] S. H. Ahn, J. H. Koh, J. A. Seo, J. H. Kim, *Chem. Commun.* **2010**, *46*, 1935.
[35] J. T. Park, D. K. Roh, R. Patel, E. Kim, D. Y. Ryu, J. H. Kim, *J. Mater. Chem.* **2010**, *20*, 8521.
[36] J. H. Koh, J. K. Koh, N. G. Park, J. H. Kim, *Sol. Energy Mater. Sol. Cells* **2009**, *94*, 436.
[37] M.-S. Kang, J. H. Kim, J. Won, Y. S. Kang, *J. Phys. Chem. C* **2007**, *111*, 5222.
[38] Y. Diamant, S. G. Chen, O. Melamed, A. Zaban, *J. Phys. Chem. B* **2003**, *107*, 1977.
[39] E. Palomares, J. N. Clifford, S. A. Haque, T. Lutz, J. R. Durrant, *J. Am. Chem. Soc.* **2003**, *125*, 475.
[40] S. A. Haque, Y. Yachibana, D. R. Klug, J. R. Durrant, *J. Phys. Chem. B* **1998**, *102*, 1745.